GEOLOGICAL SURVEY OF CANADA
OPEN FILE 7072

Firn dielectric properties derived using data from the high bandwidth (5-18 GHz) surface radar acquisitions at the Summit Camp, Devon Ice Cap, Nunavut, 2008

D.O. Burgess
L. Gray

2012

Natural Resources Canada
Ressources naturelles Canada

Canada

GEOLOGICAL SURVEY OF CANADA
OPEN FILE 7072

Firn dielectric properties derived using data from the high bandwidth (5-18 GHz) surface radar acquisitions at the Summit Camp, Devon Ice Cap, Nunavut, 2008

D.O. Burgess
L. Gray

2012

doi:10.4095/289902

This publication is available from the Geological Survey of Canada Bookstore (http://gsc.nrcan.gc.ca/bookstore_e.php).
It can also be downloaded free of charge from GeoPub (http://geopub.nrcan.gc.ca/).

Recommended citation:
Burgess, D.O. and Gray, L., 2012. Firn dielectric properties derived using data from the high bandwidth (5-18 GHz) surface radar acquisitions at the Summit Camp, Devon Ice Cap, Nunavut, 2008; Geological Survey of Canada, Open File 7072, 13 p. doi:10.4095/289902

Table of Contents

Introduction

This report is a summary of the results pertaining to the firn dielectric properties as derived from ground penetrating radar surveys conducted in support of the Calibration and Validation ESA's CryoSat-2 radar altimeter (Wingham et al. 1998). A primary mission objective of the CryoSat-2 radar altimeter is to provide important information on the rates of mass change of all land ice on the planet.

Study Site

The ground based radar experiments were conducted at the CryoSat Summit Camp on the Devon Ice Cap, Nunavut (Figure 1), in May, 2008. The summit camp is located at 1800 m a.s.l. in the percolation zone of the ice cap. The near surface structure within this glaciological zone is composed of a matrix consisting of snow, firn, saturated firn, depth hoar, and ice lenses, and has a net bulk density of 400-500 kg m^{-3}. Long-term and annual pole measurements of surface mass balance indicate that the net annual snow accumulation is 19 – 23 cm w.e. (Koerner, 2005; Burgess and Sharp, 2007).

The Ground Penetrating Radar System

The ground penetrating radar used in this study was a step-frequency radar (5 – 18 Ghz) on loan from the British Antarctic Survey. The radar consisted of an Agilent Network Analyzer installed in a temperature regulated case (Figure 2). The two horn antennae were supported by an aluminum arm and aimed at the snow surface. The radar and temperature controlled case were powered by a 2 Kw generator that was all mounted on a komatiq sled platform. An aluminum mass balance pole was used as a calibration target on the snow surface (see Figure 2) and at depth within the snow and firn pack.

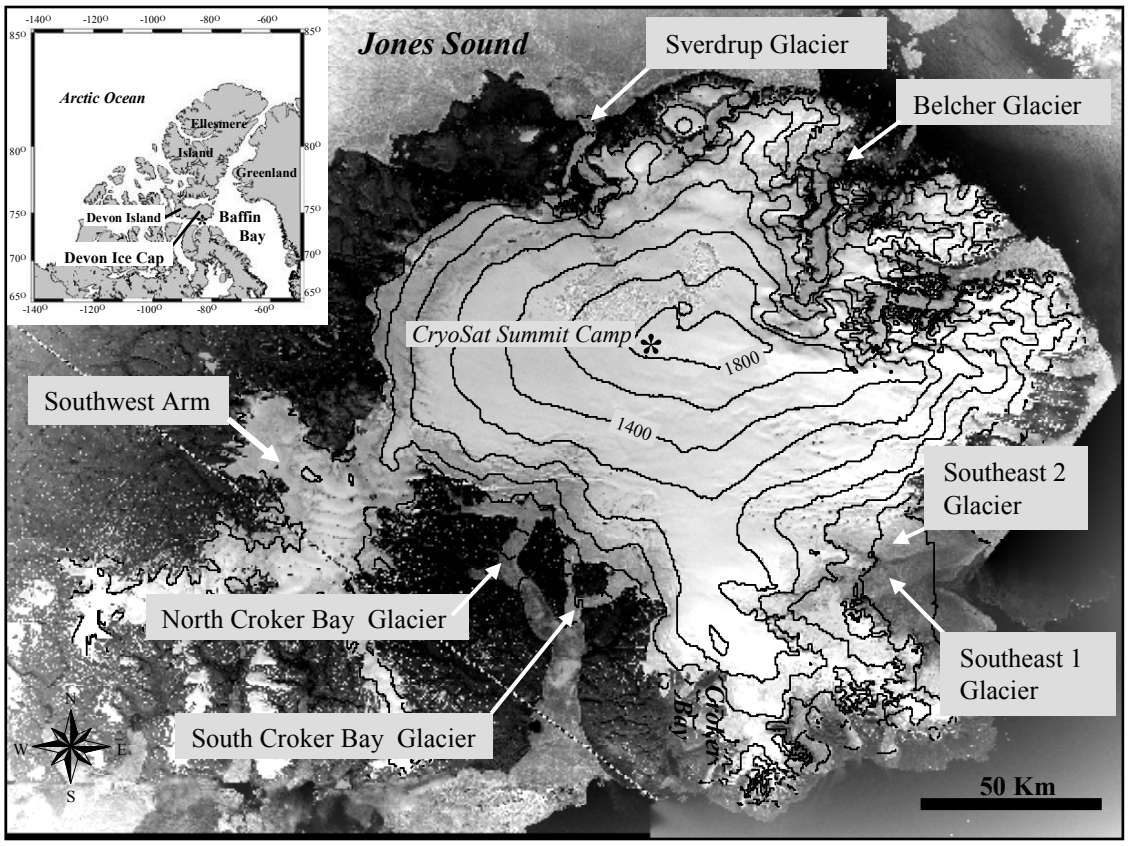

Figure 1. Location of the CryoSat Summit Camp location in central Devon Ice Cap, Nunavut. Elevations are in meters above sea-level.

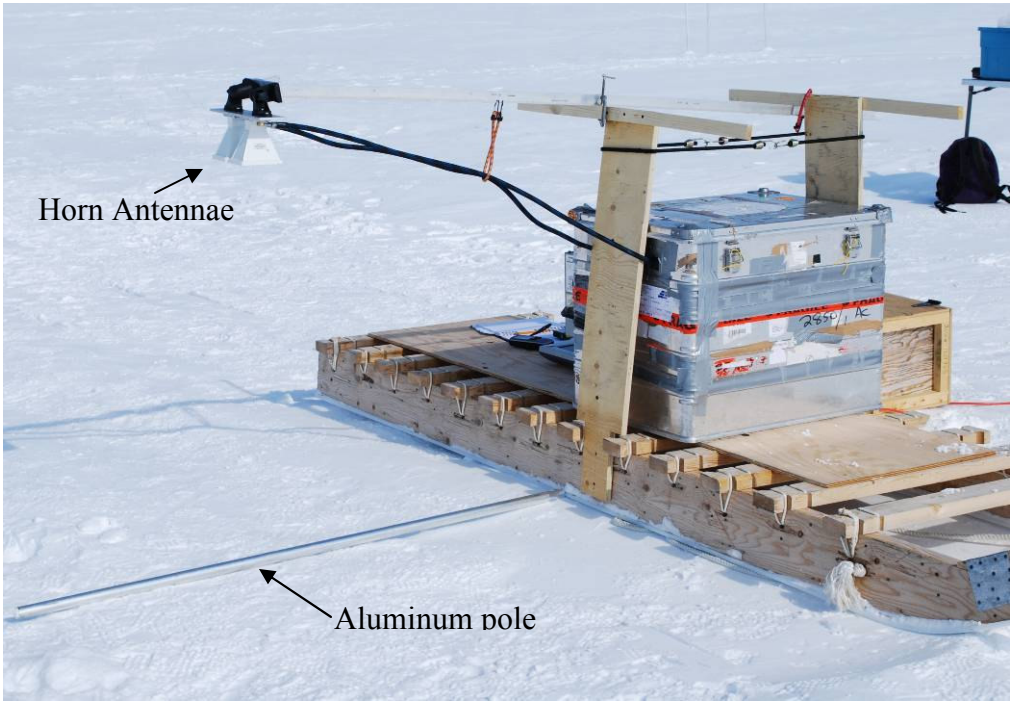

Figure 2. The high frequency ground penetrating radar mounted on a komatiq sled at the Devon Ice cap Summit Camp.

Identification of the Snow Surface

The first radar measurements were performed to identify precisely the location of snow surface in the radar signal. This was done by acquiring a radar shot with the aluminum pole positioned on the snow surface directly under the antennae (Figure 2), and a shot with no pole in the radar field of view. As can be seen in Figure 3, this exercise clearly illustrates the influence of positioning a 3.2 cm diameter pole on the surface of the snow and the very good accuracy with which the position of the surface can then be identified. The pole produces a radar shadow which affects the 'speckle' pattern for larger delay times and deeper depths. This means that the red curve will not duplicate the blue curve exactly although the patterns are clearly correlated. Note the blowup (which spans 10 cm in range) showing the remarkable resolution achieved with the 5 - 18 GHz sweep and the sub-centimeter accuracy with which the surface can be identified.

Calibration of speed of propagation in the various layers in the firn

Calibration of the propagation speed through firn was performed initially by acquiring multiple radar shots along a ~3m transect. The whole radar setup was physically moved between each of the shot so that averaging could be performed and a new spatial 'independent look' could be obtained. Data acquisition began at the south end of the calibration transect progressing northward. A pit was subsequently dug to expose the face (Figure 4) beneath the line covered by the movement of the radar antennae.

The speed of propagation data set was acquired in a section of the pit that was extended downwards to a depth of ~1.8 m. Holes for this procedure were drilled horizontally into the pit wall (Figure 5) using a 2" diameter Kovacs auger. The lowest hole (1.69 m) was drilled first, and then the radar data was acquired with and without the pole. The 5 other holes were subsequently drilled and data was acquired by alternating the pole-in pole-out routine, working from the bottom up.

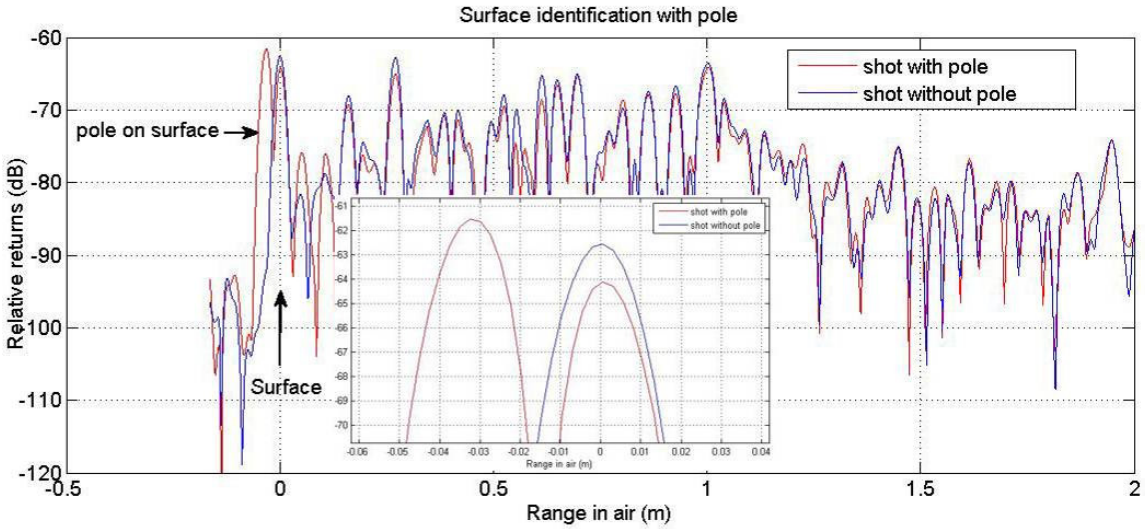

Figure 3. Example of power returns for 2 radar 'shots'. The first (blue) was acquired without the short section of the aluminum mass balance pole, and the second (red) with the pole laid on the surface.

Figure 4. Mosaic of 6 photos taken after the radar data had been acquired and the pit dug to expose the layering beneath the radar antennae. The exposed face of the pit in this photo mosaic is ~ 2.7 m long by 0.6 m high and the north end is to the right of the figure. The top two holes (H1 and H2) drilled for calibration are visible on the right and this corresponds to the near surface part (depth < 60 cm) of the pit.

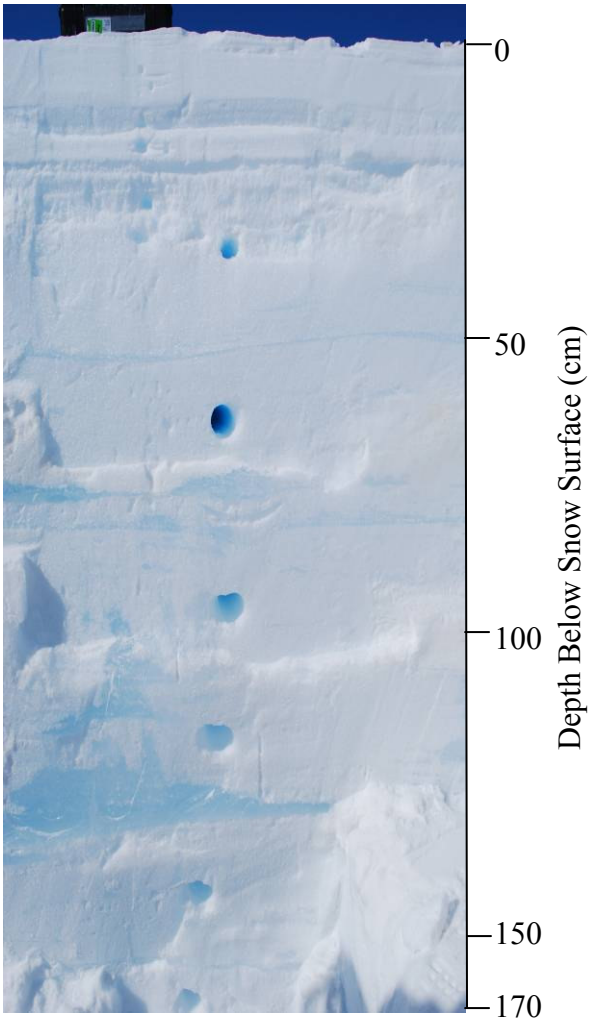

Figure 5. Photo mosaic of firn section through which radar permittivity calibration experiments were performed.

The technique used to identify the radar return from the pole when it was inserted into a hole drilled in the pit face is as follows: Data from 3 shots were recorded then the deepest hole was drilled and 2 additional shots were recorded with the pole in place. Further holes were drilled working upwards until the shallowest hole was drilled such that the top of the pole was at 29.5 cm from the surface. Results of the radar return values (db and power) are presented in Figures 6 and 7 for at least one shot without the pole (blue) and a second one with the pole (red). By presenting the return power on a log scale (dB) one can easily see when the return pattern changes. Beginning at 0 (the surface determined by using the pole on the surface) one can see the position when the blue curve appears from 'behind' the red curve; this indicates the position of the pole. By subtracting the power (not dB) without the pole from the power with the pole, a more accurate estimate of the delay time or range in air can be made for the near surface holes. Figure 6 shows the range in air to the pole is 35.0 cm but the physical distance is 29.5 cm. Similarly, Figure 7 shows the range in air to the pole is 76.2 cm but the physical distance is 56 cm. Data from the deeper holes is not as clear as those illustrated above, and results from the deepest hole at 1.69 m were difficult to interpret and thus not included in the results shown in Table 1.

When viewed as a continuous scale for the entire pit depth, the results show a clear relationship between the density and permittivity (Figure 8). As the density varies over a relatively wide range (from the difficult-to-measure density of the weak hoar frost layers to the pure ice layers that can exist from summer melt) so also will the speed of propagation. Using a straightforward interpolation one can see the scale tags on the right-hand scale in Figure 8 come closer together when the density increases (eg. at 170 cm depth), implying a decrease in propagation speed.

Time domain traces from full resolution (5 – 18 GHz) processing of the individual shots have been placed side-to-side to create a delay-time reflectivity pseudo image along part of the calibration pit (Figure 9). The pseudo image clearly highlights continuous layers (as thin as 1cm) within the near surface firn to an actual depth of ~40 cm below the snow surface.

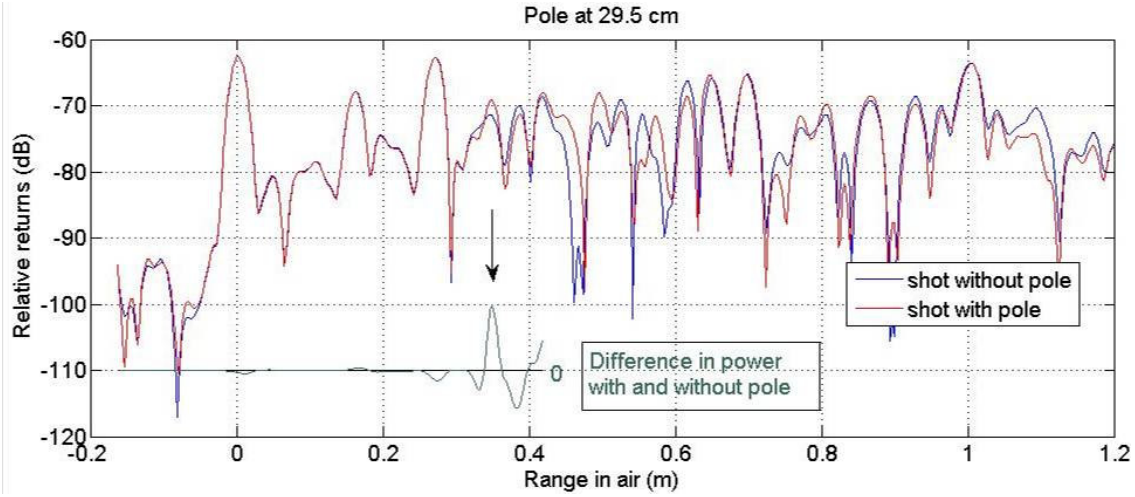

Figure 6. Radar return (db and power) with and without the pole inserted into the top hole at 29.5 cm from the surface.

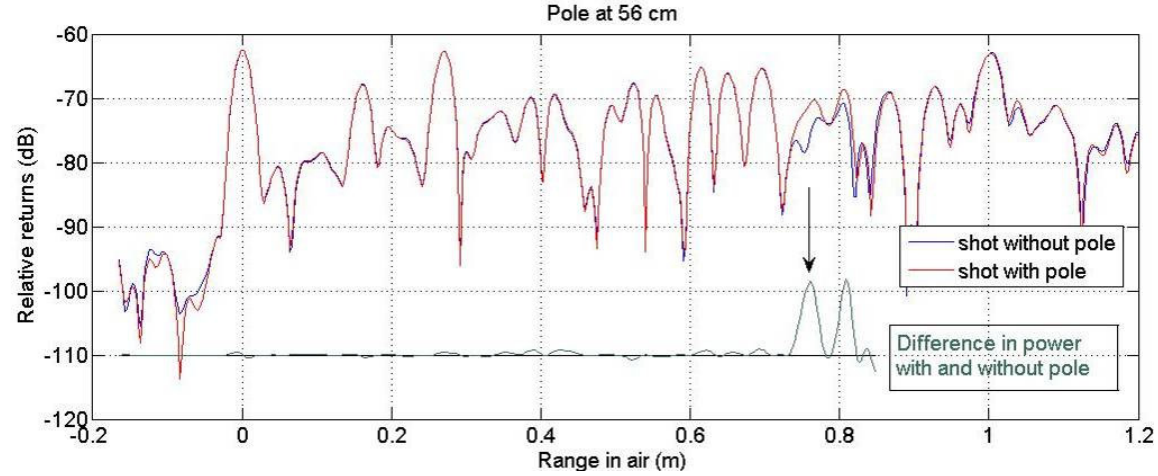

Figure 7. Change in return (db and power) with and without the pole inserted with the pole at 56 cm from the surface.

Table 1. Estimates of the average relative permittivity obtained by measuring the time delay between the surface and the metal pole, and then using the measured physical distance between the surface and top surface of the pole to estimate the average refractive index and thereby the relative permittivity and speed of propagation.

Surface to…	Physical distance (cm)	Measured Range (cm)	Average Refractive Index	Average relative permittivity	Average Propagation speed. (m/ns)
Hole 1	29.5	34.8 ± 0.6	1.18 ± 0.02	1.39 ± 0.05	0.254 ± 0.004
Hole 2	56	76.2 ± 1	1.36 ± 0.02	1.85 ± 0.05	0.221 ± 0.004
Hole 3	86	118 ± 3	1.37 ± 0.03	1.88 ± 0.08	0.219 ± 0.005
Hole 4	109	148 ± 3	1.36 ± 0.03	1.85 ± 0.08	0.221 ± 0.005
Hole 5	142	200 ± 5	1.41 ± 0.04	2.02 ± 0.11	0.217 ± 0.006

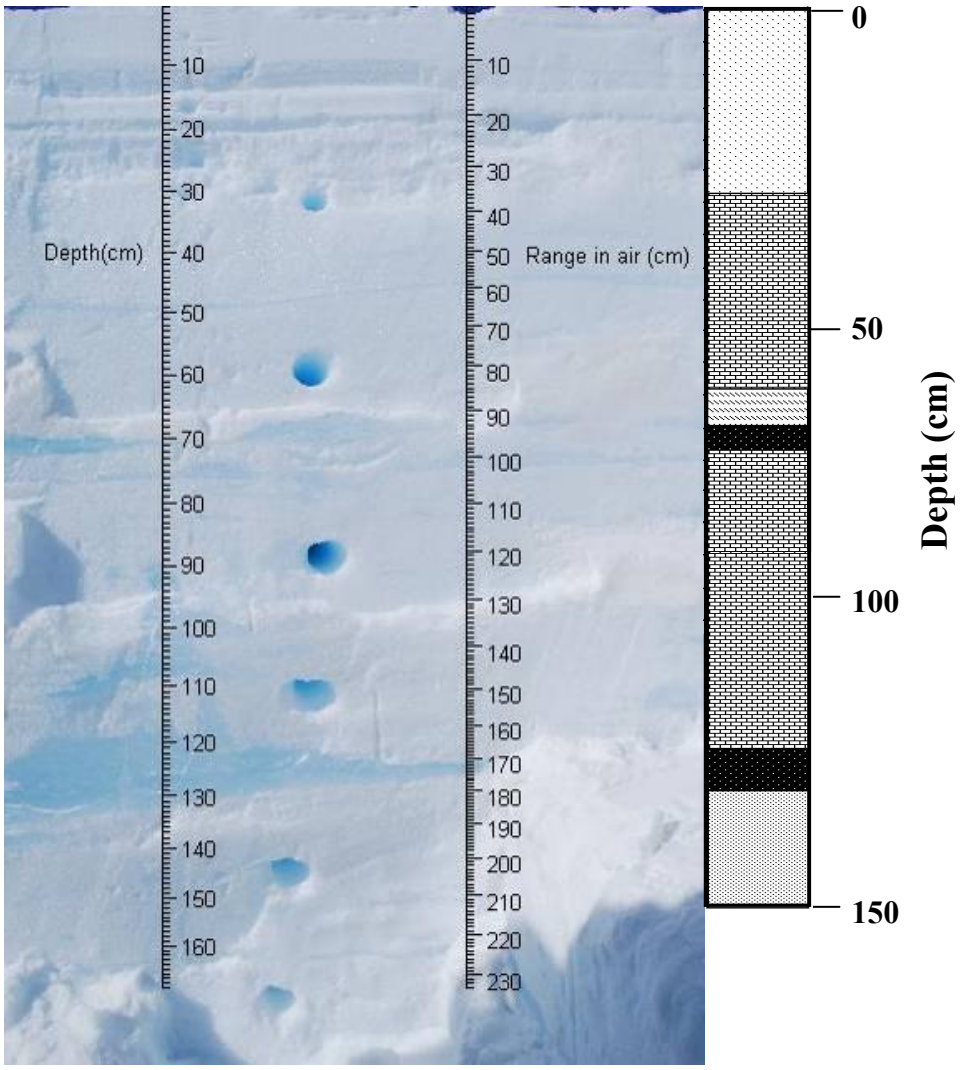

Figure 8. Photo mosaic of the calibration pit wall, schematic of the stratigraphy, and density of the major stratigraphic units (depth in cm) along the column. The vertical distance scale (left) and equivalent radar range in air (right) are superimposed on the photo mosaic. The close spacing of the millimeter scale gradations on the right hand scale gives an indication of the slower propagation speed through the denser firn and ice. Firn stratigraphy (along right-hand side of photomosaic) was logged from a section ~2 m north of the calibration column.

a)

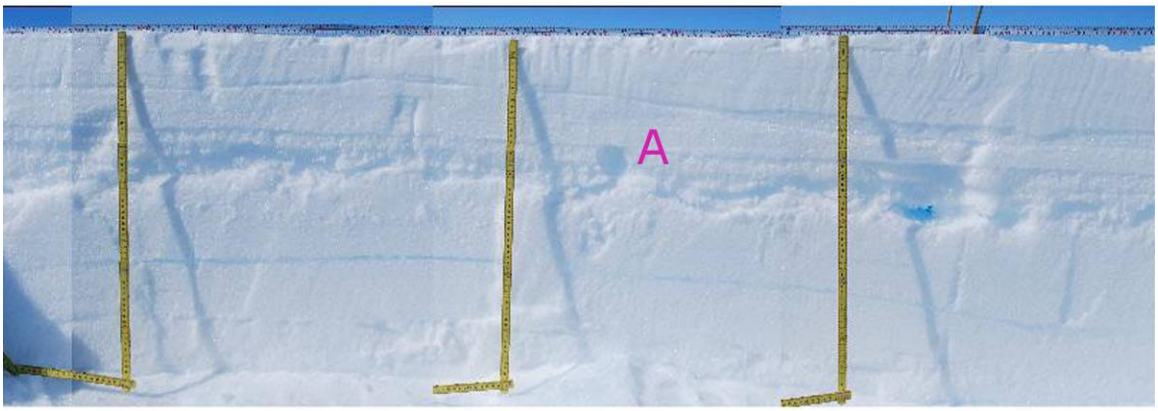

b)

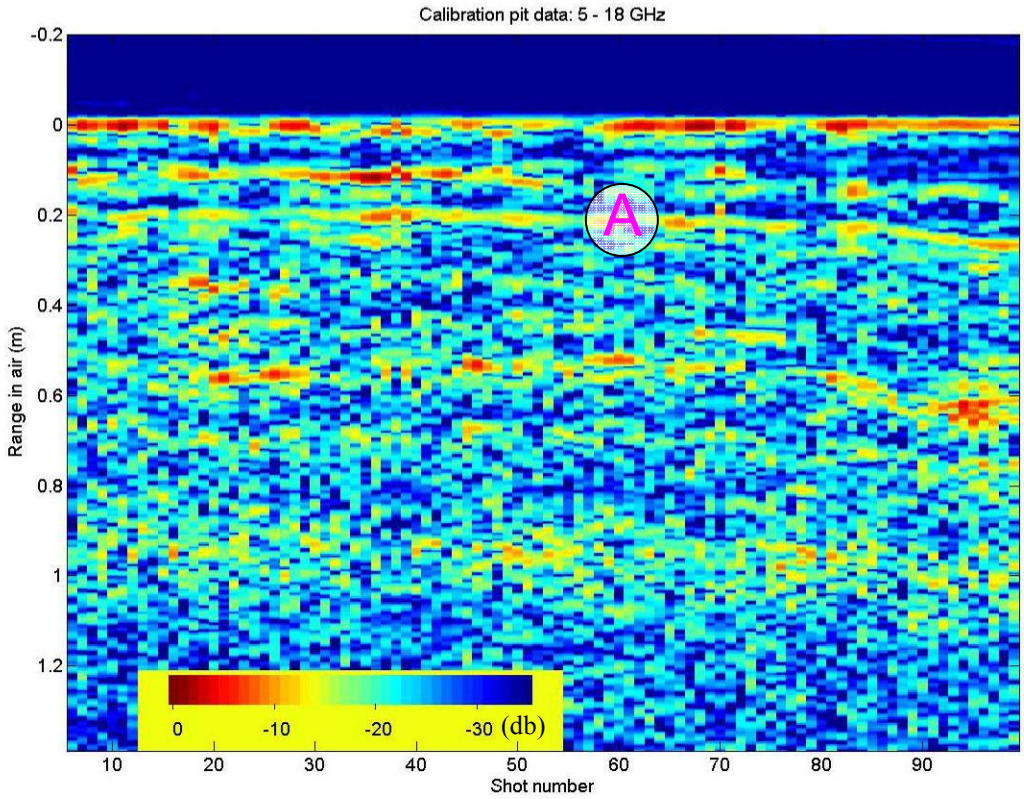

Figure 9. **(a)** A mosaic of 3 hand-held photos of part of the wall of the calibration pit. The bend in the meter scale is at the 60 cm mark. **(b)** The full resolution radar data for a sequence of 99 shots where the radar was moved ~ 2 cm between each shot. The density interface at 'A' in the photo mosaic **(a)** leads to a strong reflection shown again as 'A' in the time domain radar results **(b)**.

Summary

Investigations of the behavior of Ku-band radar energy and the near surface firn were performed near the summit of the Devon ice cap, Nunavut. Results from this study indicate a speed of the high frequency (5-18 Ghz) radar signal to range from 0.217 – 0.254 nm s^{-1} within ~2 m of the ice cap surface. Close analysis of data revealed that the speed of the radar signal decreases (increases) significantly as it passes through higher (lower) density units of the firn column. In addition, enhanced return power generated from subsurface layer boundaries where density changes are sharp, permit accurate mapping of reflecting horizons to depths of ~60 cm below the ice cap surface. Results from these experiments provide an important step towards proper interpretation and calibration of air- and space-borne Ku-band radar altimetry data over high latitude percolation zone surfaces.

References

Burgess, D.O., and M.J. Sharp. 2008. Recent changes in thickness of the Devon Island ice, Canada. *Journal of Geophysical Research,* **113,** doi:10.1029/2007/JB005238.

Wingham, D.J., Johannessen, O., Lemke, P., Tscherning, C., Picardi, G., Sandven, S., Vaughan, D., Laxon, S. and R. Scharroo, 1998. CryoSat: Response to the ESA Earth Explorer Opportunity Mission AO, UCL

Koerner, R.M. 2005. Mass balance of glaciers in the Queen Elizabeth Islands, Nunavut, Canada. *Ann. Glaciol.,* **42**, 417–423.